

## PARTICLE HEATING BY NONLINEAR ALFVÉNIC TURBULENCE IN ADAFS

MIKHAIL V. MEDVEDEV<sup>1</sup>

Harvard-Smithsonian Center for Astrophysics, 60 Garden St., Cambridge, MA 02138

*Draft version December 18, 2018*

### ABSTRACT

Particle heating in advection-dominated accretion flows (ADAFs) by nonlinear MHD (Alfvénic) turbulence is investigated. Such turbulence with highly-fluctuating magnetic fields,  $\tilde{B} \sim B_0$ , is believed to be naturally produced by the magnetic shearing instability near the nonlinear saturation. It is shown that the energy is dissipated in the parallel cascade, which occurs due to nonlinear compressibility of high-amplitude turbulence, and predominantly heats protons, but not electrons. The conservative limit on the electron-to-proton heating fraction is  $\delta \lesssim \text{few} \times 10^{-2}$ .

*Subject headings:* accretion, accretion discs — MHD — plasmas — turbulence — waves

### 1. INTRODUCTION

The Advection-Dominated Accretion Flows (ADAFs) are a class of hot, optically thin accretion solutions (Ichimaru 1977; Rees et al. 1982; Narayan & Yi 1995; Abramowitz et al. 1995; see e.g., Narayan, Mahadevan, & Quataert 1998 for review) which describe quite well the spectral characteristics of a number of low luminosity accreting black hole systems, e.g., black hole binaries (Narayan, Barret, & McClintock 1997; Hameury et al. 1997) and low luminosity galactic nuclei (e.g., Sgr A\*: Narayan, Yi, & Mahadevan 1995; Manmoto et al. 1997; Mahadevan 1998; Narayan et al. 1998; NGC 4258: Lasota et al. 1996; Gammie, Narayan, & Blandford 1999; M87 and other ellipticals: Reynolds et al. 1996; Mahadevan 1997; Di Matteo et al. 1999). In ADAFs, the protons and electrons are thermally decoupled (Coulomb collisions are rare), so that all the energy generated by turbulent viscous stresses is stored as thermal energy of the protons and ultimately advected beyond the black hole horizon, while the electrons remain relatively cool and radiate much less energy, hence the sub-Eddington luminosities. In such hot accretion flows, however, the particle mean free path is often comparable to the size of the system, and thus collective plasma effects are likely to be significant (Rees et al. 1982).

In the absence of collisions, strong MHD turbulence is required for the angular momentum transport and energy dissipation in accretion flows. The way MHD turbulence dissipates in hot accretion flows turns out to be crucial for the relevance of ADAF models. Let's denote  $P_e$  and  $P_p$  the amounts of energy that heat the electrons and protons, respectively. In traditional ADAF models, the branching ratio parameter  $\delta = P_e/P_p$  is commonly assumed to be less than or similar to  $10^{-2}$ . The predicted spectra are only weakly sensitive to the exact value of  $\delta$  so long as  $\delta \lesssim 10^{-2}$ , while for larger values of  $\delta$  the changes in spectrum characteristics are drastic because the electrons become hot and radiate a large fraction of the internal energy of the flow via the synchrotron emission so that the flow is no longer advection-dominated. The above constraint on the value of  $\delta$  has been recently relaxed in the modified ADAF

model with wind outflows (Blandford & Begelman 1999). Because of the lower accretion rates (due to the mass loss) at the inner regions, where most of the radiation is produced, the density of the inflowing gas and the magnetic field strength decrease (assuming constant  $\beta$ ) and result in a much lower radiative efficiency of the flow. It was demonstrated by Quataert & Narayan (1999) that the values of  $\delta$  as high as  $\delta \sim 0.3$  are still plausible in the advection-dominated flows with strong winds. The question of turbulent particle heating and non-thermal coupling of electrons and protons in hot accretion flows has been addressed in several works (Quataert 1998; Quataert & Gruzinov 1999; Bisnovaty-Kogan & Lovelace 1997; Begelman & Chiueh 1988; Narayan & Yi 1995). To proceed further, we need to understand what type of MHD turbulence is most likely to be realized in ADAFs.

It is commonly believed that MHD turbulence in accretion flows is generated by the magneto-rotational instability (Balbus & Hawley 1991), which generates the large-scale magnetic field as well as produces random gas motions and strong fluctuating magnetic fields in the nonlinear regime. Hence, a variety of plasma waves may be generated. Only low-frequency waves may be efficiently excited by large scale motions and carry a significant fraction of the turbulent energy. Quataert (1998) shows that among the low-frequency MHD waves, fast and slow magnetosonic waves are strongly damped in the two-temperature  $T_p \sim 10^{12}$  K,  $T_e \sim 10^9$  K ( $T_p$  and  $T_e$  are the proton and electron temperatures) ADAF plasma by collisionless dissipation (known as Landau damping and its magnetic analog the transit time damping) while Alfvén waves are still very weakly damped in the incompressible approximation. As argued by Quataert (1998), the “impedance mismatch” will likely inhibit excitation of heavily damped modes and thus the MHD turbulence in ADAFs will be (predominantly) *Alfvénic*. Additionally, it is natural to believe that the turbulent fluctuating magnetic fields are of order of the mean, large scale magnetic field,  $\tilde{B} \sim B_0$ , and the Balbus-Hawley instability is nonlinearly saturated.

A detailed study particle heating processes by Alfvénic

<sup>1</sup>Also at the Institute for Nuclear Fusion, RRC “Kurchatov Institute”, Moscow 123182, Russia; E-mail: mmedvedev@cfa.harvard.edu; URL: <http://cfa-www.harvard.edu/~mmedvedev/>

turbulence in ADAFs neglecting the effects of compressibility has been performed by Quataert (1998) and Quataert & Gruzinov (1999). They assumed that the energy which is injected into the system on large scales comparable to the size of the accretion flow,  $L \sim R$ , will cascade in  $k$ -space to small scales, typically the proton Larmor scale,  $l \sim \rho_p = v_{\text{th}p}/\Omega_p$  (with  $v_{\text{th}}$  being the thermal particle velocity and  $\Omega = eB_0/mc$  being the cyclotron frequency) or even smaller, where it dissipates. Since the Alfvén wave cascade is likely anisotropic (Goldreich & Sridhar 1995), the  $k$  components are related as  $k_{\parallel} \sim k_{\perp}^{2/3} L^{-1/3}$ . Thus, when the cascade reaches  $k_{\perp}$  such that  $k_{\perp} \rho_p \sim 1$ , the wave energy dissipates only via Landau damping (Cherenkov resonance) and may preferentially heat either the electrons or the protons, depending on the value of plasma  $\beta$  ( $\beta = 8\pi p/B_0^2$  is the ratio of gas to magnetic pressure).<sup>2</sup> The cyclotron damping which may be very efficient to heat protons is unimportant in this case, because  $k_{\parallel} \ll k_{\perp}$  and  $\omega = k_{\parallel} v_A \ll \Omega_p$  (where  $v_A^2 = B_0^2/4\pi m_p n$  is the Alfvén speed and  $n$  is the particle density), so that the cyclotron resonance ( $\omega - k_{\parallel} v - \Omega_p = 0$ ) is satisfied for a negligibly small population of very energetic particles from the tail of the Maxwellian distribution function. Quataert & Gruzinov (1999) also argue that only a fraction of Alfvénic energy may be dissipated on the scale  $k_{\perp} \sim \rho_p^{-1}$  and the rest of it passes this ‘barrier’. On scales  $k_{\perp} \gg \rho_p^{-1}$  Alfvén waves may be converted to whistler waves and cascade even further where dissipation on electrons may be dominant. Because the details of how Alfvén waves are converted into whistler waves on scales  $k_{\perp} \sim \rho_p^{-1}$  are not known, they estimate that the transition from the electron dominated heating regime to the proton dominated one occurs somewhere inbetween  $\beta \sim 5$  and  $\beta \sim 10^2$ .

The above analysis is accurate for low-amplitude turbulence,  $\tilde{B}/B_0 \ll 1$ , where one can neglect the effect of finite magnetic field pressure,  $\tilde{B}^2/8\pi$ , (i.e., incompressible plasma) and use the linear theory. In a high-amplitude turbulence,  $\tilde{B}/B_0 \sim 1$ , which is likely to be present in accretion flows, finite magnetic pressure of waves nonlinearly couples Alfvénic energy to ion-acoustic-like (i.e., density) quasi-mode perturbations, which are, in general, dissipative. In this paper, we show that:

1. The Alfvénic *parallel* cascade towards higher  $k_{\parallel}$  exists in a compressible MHD turbulence as a result of nonlinear wave steepening (modulational instability), in addition to the perpendicular (incompressible) cascade in  $k_{\perp}$ . This parallel cascade is nonlinearly dissipative because it proceeds via the excitation of ion-acoustic (i.e., compressible) quasi-modes which are damped via the Landau mechanism. Even for relatively small amplitudes of turbulence,  $\tilde{B}/B_0 \gtrsim 0.2$ , and for  $\beta \gtrsim 3$ , much or almost *all* magnetic energy of Alfvén waves dissipates before it reaches the perpendicular ‘dissipation barrier’,  $k_{\perp} \rho_p \sim 1$ . The perpendicular cascade, thus, turns out to be energetically unimportant. Dissipation in the nonlinear parallel cascade preferentially

heats the protons and yields  $\delta \lesssim \text{few} \times 10^{-2}$ .

2. If  $\beta \lesssim 3$ , the turbulence bifurcates to another ‘phase’ where the Alfvénic dissipation in the parallel cascade is weak and other dissipation mechanisms (at small scales) are required to maintain a steady-state. Since the parallel cascade proceeds up to  $k_{\parallel} \simeq 4(\tilde{B}/B_0)(\Omega_p/v_A)$ , the Alfvénic turbulent energy may be efficiently dissipated due the cyclotron damping on protons, if  $\omega = k_{\parallel} v_A \simeq \Omega_p$ , i.e., if  $\tilde{B}/B_0 \gtrsim 0.3$ . Only protons may be heated in this regime. For lower amplitudes, the perpendicular Goldreich-Sridhar cascade is likely to dominate and energy dissipates, as discussed by Quataert (1998) and Quataert & Gruzinov (1999). The three-wave cascade (Ng & Bhattacharjee 1996), if it dominated the above four-wave cascade, turns out to be insignificant for electron energetics.

We also consider other ‘higher-order’ nonlinear effects, such as particle trapping, and their relevance to particle heating in ADAFs.

The paper is organized as follows. In §2 we discuss the noisy-KNLS model of strong MHD turbulence. In §3 we apply the model to the conditions in ADAFs. We compare the model at hand with other competing turbulent processes in §4. Section §5 is the conclusion.

## 2. THE MODEL OF NONLINEAR ALFVÉN WAVE TURBULENCE

### 2.1. General considerations

It is known that in an incompressible plasma,  $\nabla \cdot \mathbf{v} = 0$ , the Reynolds and magnetic stresses (i.e., the fluid and magnetic nonlinearities) in a finite-amplitude Alfvén wave cancel each other exactly. Such a wave behaves as if it is linear. Hence, only the Goldreich-Sridhar Alfvénic perpendicular,  $k_{\perp}$ , cascade occurs in a turbulent regime. The mutual cancellation of Reynolds and magnetic stresses in the wave breaks down when plasma is compressible. Indeed, the magnetic field pressure,  $\tilde{B}^2/8\pi$ , associated with the wave field exerts an additional stress onto an ionized gas and change its local density,  $n$ . Variations in  $n$  affect, in turn, the local wave phase speed,  $v_A$ , and introduce a positive nonlinear feedback into the wave dynamics (Cohen & Kulsrud 1971). This nonlinear phase speed–amplitude coupling in *nonlinear Alfvén* waves results in the *modulational instability* which is ultimately responsible for the wave-front steepening, parallel,  $k_{\parallel}$ , Alfvénic cascade, and formation of collisionless shocks. The compressional nonlinearity may also be viewed as an effective parametric coupling of a finite-amplitude Alfvén wave to ion-acoustic (i.e., density) wave-like perturbations in a medium.<sup>3</sup> These ion-acoustic quasi-modes are compressional and have a longitudinal component of the electric field (with respect to the ambient magnetic field). Hence, they efficiently dissipate the energy via Landau damping. A quantitative theory of nonlinear Alfvén waves is now well established (see a short review by Medvedev 1999 and references therein). Note that the dissipation of the finite-amplitude Alfvén waves

<sup>2</sup>The plasma physics  $\beta$  used in this paper is different from that used in ADAF models and is related to it as  $\beta_{\text{adaf}} = \beta/(\beta + 1)$ .

<sup>3</sup>Such ion-acoustic modes are *not* plasma eigenmodes. They are driven by the Alfvén wave and, hence, propagate with the Alfvén speed, which is, in general, different from the sound speed in plasma.

is intrinsically nonlinear process and leads to a number of unusual properties of such waves (Medvedev 1999).

## 2.2. The model

There is only one (to our knowledge) model of strong nonlinear Alfvén wave turbulence in a compressible plasma which self-consistently includes the effects of wave nonlinearity and particle kinetics, e.g., Landau damping (Medvedev & Diamond 1997). It is formulated as a stochastic modification of the dynamic equation of Alfvén waves, — the kinetic nonlinear Schrödinger equation (KNLS). This model of turbulence, referred to as the “noisy-KNLS,” is thus structure-based, meaning that it describes the turbulence as a collection of strongly interacting *coherent* structures, such as shocks, solitons, cnoidal waves, rotational discontinuities, etc., generated by an external random noise source.<sup>4</sup> The noisy-KNLS equation is

$$\frac{\partial b}{\partial \tau} + v_A \frac{\partial}{\partial x} \left( N_1 b |\widetilde{b}|^2 + N_2 b \hat{\mathcal{H}}[|\widetilde{b}|^2] \right) + i \frac{v_A^2}{2\Omega_p} \frac{\partial^2 b}{\partial x^2} = \tilde{f}, \quad (1)$$

where  $\hat{\mathcal{H}}$  is the *integral operator*, referred to as the Hilbert operator (or the Hilbert integral transform), acting on the wave field:

$$\hat{\mathcal{H}}[|\widetilde{b}|^2] = \frac{1}{\pi} \int_{-\infty}^{\infty} \frac{\mathcal{P}}{(x' - x)} |b(x')|^2 dx'. \quad (2)$$

Here also  $b = (\tilde{B}_y + i\tilde{B}_z)/B_0$  is the normalized complex wave magnetic field,  $|\widetilde{b}|^2 = |b|^2 - \langle |b|^2 \rangle$  is the fluctuating component of the magnetic pressure,  $\langle \dots \rangle$  means appropriate averaging over the spatial domain,  $\mathcal{P}$  means principal value integration,  $\tilde{f}$  is the random (turbulent) noise, and the coefficients  $N_1$  and  $N_2$  are complicated functions of parameters of a plasma and are discussed below.

The first nonlinear term in equation (1) describes the nonlinear (ponderomotive) coupling of finite-amplitude Alfvén waves to ion-acoustic modes. Indeed, the first two terms are similar to a continuity equation for the wave magnetic field,  $\partial_\tau b + \partial_x(ub) = 0$ , where the “hydrodynamic” velocity,  $u$ , is generated by the wave pressure,  $u \propto v_A |\widetilde{b}|^2$ . The process of nonlinear steepening stops when it is balanced by linear Alfvén wave dispersion which occurs at very small scales comparable to proton’s Larmor radius,  $k_\parallel \sim \rho_p^{-1}$ , as represented by the last, linear in  $b$ , term. The second nonlinear term in equation (1) describes Landau (i.e., collisionless) damping of the induced density perturbations, not the magnetic fluctuations. This collective kinetic effect is represented by the integral Hilbert operator. We emphasize that the damping is *nonlocal* which can be interpreted as the effect of particle “memory” which is associated with particle transit through the wave packet. Another interesting and important feature is the absence of any particular scale beyond which the damping dominates. Indeed, the Fourier representation of the Hilbert operator  $\hat{\mathcal{H}}[f]$  acting on a function  $f$  is  $(ik_\parallel/|k_\parallel|)f_k \equiv i \text{sgn}(k_\parallel) f_k$ , i.e., independent of

the magnitude of  $k_\parallel$ . Thus, Landau damping of nonlinear Alfvén waves occurs at all scales; it is *scale invariant*. We should comment that both nonlinearities result in the wave steepening and formation of sharp fronts (shocks) which is, practically, equivalent to the parallel cascade of wave energy to smaller scales. Unlike the conventional, incoherent cascade paradigm, however, this cascade proceeds through random interactions of coherent wave structures (such as shocks, nonlinear waves, etc.). Hence, collective wave–particle interactions, such as the nonlinear Landau damping and particle trapping also contribute.

We now briefly discuss basic assumptions used in the noisy-KNLS model. First, equation (1) is the *envelope* equation. That is, Alfvén waves themselves (carrier waves) are assumed to be linear and, thus, obey the dispersion  $\omega = k_\parallel v_A$  while the amplitude of these waves may vary in space and time and is described by equation (1). The time variable  $\tau$  is the “slow” time of the large-scale dynamics of the wave envelope,  $\tau = (B_0/\tilde{B})^2 t_A$ , where  $t_A = \omega^{-1}$  is the typical “Alfvénic” time. It has been assumed in derivation that  $(\tilde{B}/B_0)^2$  is small but finite. Comparison of the predictions of this model with observations of nonlinear Alfvén waves in the solar wind by spacecrafts shows that the KNLS theory is “robust” and supports its validity even on the margin of applicability,  $(\tilde{B}/B_0) \simeq 1$ .

Second, the noisy-KNLS also assumes that waves are propagating in one direction, only. The existence of counter-propagating waves allows for another type of parametric wave–wave interactions, — the decay instability, due to which an Alfvén wave may decay into an acoustic wave and a counter-propagating Alfvén wave, — which greatly complicates any analytical treatment of the problem. The decay instability, however, may be greatly suppressed in hot, two-temperature ADAF conditions. An acoustic (compressible) wave that is to be generated is heavily damped by collisionless dissipation. The same argument that the “impedance mismatch” inhibits resonant excitation of strongly damped modes suggests here (but does not prove, though) that the parametric resonance discussed above will be inefficient.

Third, the KNLS-based theory considers planar waves, only. That is, no wave packet modulations are allowed in the plane perpendicular to the direction of wave propagation; the wave fronts are always flat. The dynamics of waves is, thus, purely one-dimensional. This strong limitation of the dynamics and evolution of wave structures in the Alfvénic turbulence has, probably, very little effect (if any) on the processes of particle heating. Indeed, on large scales, particles move along field lines, only. Thus, heating of particles may occur (in Cherenkov resonance) via increase of their parallel velocity, only. The perpendicular wave evolution, therefore, hardly affects particle energy, unless  $k_\perp \sim \rho_p^{-1}$ . Note, the effective one-dimensionality of the problem does not mean that waves may propagate along the ambient magnetic field,  $\mathbf{B}_0$ , only. It has been shown that waves propagating at angle are still described by equation (1) if one formally writes the wave field as  $b = (\tilde{B}_y + B_0 \sin \Theta + i\tilde{B}_z)/B_0$ , where  $\Theta$  is the angle<sup>5</sup> be-

<sup>4</sup>In this respect, the model is analogous to the noisy-Burgers model of hydrodynamic turbulence which describes the turbulence as a collection of randomly interacting collisional shocks.

<sup>5</sup>Strictly speaking, the angle  $\Theta$  cannot be pushed close to  $90^\circ$  because dispersion becomes different for left-hand- and right-hand-polarized waves (dispersion on electrons vs. dispersion on protons). This sets the limit on the angle  $(\pi/2 - \Theta) \gg \sqrt{m_e/m_p}$ .

tween  $\mathbf{k}$  and  $\mathbf{B}_0$ .

Fourth, the nonlinear coupling coefficients,  $N_1$  and  $N_2$ , presented in the Appendix are calculated by solving the particle kinetic (Vlasov) equation (Spangler 1989, 1990) and agree with those calculated using the guiding center formalism (Mjølhus & Wyller 1988). Both methods, however, used perturbative techniques and do not include nonlinear effects such as particle trapping. Maxwellian distribution was assumed for bulk particles. Gruzinov & Quataert (1999) showed that in a strong Goldreich-Sridhar turbulence the time-asymptotic distribution function of protons may be different. It is not clear whether this situation occurs in ADAF because (i) the infall (accretion) time may be shorter than the velocity diffusion time required to establish a new distribution and (ii) the emergent distribution should, in general, be anisotropic (because the turbulence is anisotropic) and thus may be unstable against, for instance, fire-hose instability which will isotropize and thermalize the particles. Since Landau damping is a resonant process, it cares about the local slope of a distribution function, but its overall shape is irrelevant. Therefore, using the Maxwellian distribution is reasonable.

Finally, we do not specify the origin of random forcing for the moment. In general, involvement of a particular mechanism would force re-ordering in equation (1) and changes in  $N_1$  and  $N_2$ . This complication is automatically eliminated in the renormalization-group approach, the key idea of which is to use bare nonlinear couplings to compute the noise-renormalized (i.e., turbulent) quantities (Medvedev & Diamond 1997). Going ahead, the reason why the bifurcation point (see next section) seems to be determined by the bare  $N$ 's and not the turbulent ones is simple: both nonlinearities are cubic and renormalize in the same way.

### 2.3. The structure of Alfvénic turbulence

We are interested in a steady-state turbulence in which the energy input due to random forcing is balanced by Landau dissipation. Since this dissipation is independent of  $|k|$ , it occurs at *all scales*; thus, no inertial interval exists. An analytical study of the model for arbitrary noise is an extremely laborious task. That is why it has been analyzed only in the simplest case of  $\delta$ -correlated in space and time, zero-mean, white in  $k$  noise (Medvedev & Diamond 1997). A one-loop renormalization group technique has been utilized. The noise-dependent renormalized turbulent transport coefficients has been obtained. Quite importantly, they are mostly determined by properties of the noise source on the largest scales (i.e., the system size), — the so called infrared divergences. The large- $k$  tail of the noise spectrum seems to be relatively insignificant to control global properties of turbulence. Thus, the assumption of white noise is likely to be unproblematic in the context of turbulence in hot accretion flows, because the spectrum of turbulence is not known, anyway.

The existence of two distinct *phases* (or regimes) of compressible Alfvénic turbulence constitutes the most important and interesting prediction of the theory. The system will *bifurcate* (rather than smoothly transit) from one phase to another, as plasma parameters smoothly change. The bifurcation point is determined by the ratio of the

nonlinearity-to-damping coefficients:

$$\left. \frac{|N_1|}{|N_2|} \right|_{\text{bif}} \simeq 1.3. \quad (3)$$

This result has been obtained rigorously from the analysis of the self-consistency of the infrared cutoff scalings of the solutions for turbulent transport coefficients. The physical interpretation, however, is very simple and clear. If  $|N_1|/|N_2| < 1.3$ , the collisionless dissipation always dominates the nonlinear parallel energy cascade (i.e., the wave steepening). Most of the energy injected on a large scale dissipates *before* it reaches the dispersion scale, and *all* the energy is dissipated *via* Landau damping in the Alfvénic cascade. Thus, the steady-state, so-called “hydrodynamic” ( $\omega, k \rightarrow 0$ ) turbulence with no steep fronts is predicted. In the opposite case  $|N_1|/|N_2| > 1.3$ , no mathematically rigorous prediction can be made, since no solution to renormalized equations exists. Speculatively, however, it is clear that the collisionless damping is weak compared to the nonlinear steepening. Only a small fraction of the injected energy dissipates, while most of it cascades along  $k_{\parallel}$  to the smallest scales set by the linear dispersion. Since the source continuously injects energy into the system, it will be *accumulated* at the smallest scales. Hence, a non-steady-state, small-scale turbulence of Alfvénic shocklets is expected. Stationarity may be enforced by including other dissipation mechanisms into the model. The most efficient one is the cyclotron damping on protons because it operates at nearly the same scales (i.e., the proton Larmor radius) where the wave energy is accumulated. Another mechanism which dominates for linear and weakly nonlinear waves ( $\tilde{B}/B_0 \ll 1$ ) is the perpendicular cascade (Goldreich & Sridhar 1995; Ng & Bhattacharjee 1996). The energy may cascade through  $k_{\perp} \sim \rho_p$  to smaller scales where Alfvén waves are probably converted into whistler waves. How energy is dissipated in this case is unclear (Quataert & Gruzinov 1999). The discussion of these issues and quantitative estimates of the rates of the perpendicular vs. parallel cascade and cyclotron damping are given in §4.

## 3. APPLICATION TO HOT ACCRETION FLOWS

### 3.1. Preliminary notes

In this section, we primarily focus on the ADAF solutions which are the only known thermally stable, self-consistent models of hot, two-temperature accretion flows. The self-similar scalings of plasma parameters relevant for our problem are (Narayan & Yi 1995, see also Quataert 1998):

$$T_p \simeq 2 \times 10^{12} \frac{\beta}{\beta + 1} r^{-1} \text{ K}, \quad (4a)$$

$$T_e \sim 10^9 - 10^{10} \text{ K}, \quad (4b)$$

$$\beta = \text{const.}, \quad (4c)$$

$$B_0 \simeq 10^9 \alpha^{-1/2} (1 + \beta)^{-1/2} m^{-1/2} \dot{m}^{1/2} r^{-5/4} \text{ G}, \quad (4d)$$

$$\frac{\rho_p}{R} \simeq 6 \times 10^{-9} \alpha^{1/2} \beta^{-1/2} m^{-1/2} \dot{m}^{-1/2} r^{-1/4}, \quad (4e)$$

$$\frac{v_A}{c} \simeq 0.9(1 + \beta)^{-1/2} r^{-1/2}, \quad (4f)$$

$$\frac{v_r}{c} \simeq 0.37 \alpha r^{-1/2}, \quad (4g)$$

where  $\alpha$  is the Shakura-Sunyaev turbulent viscosity parameter,  $m = M/M_\odot$  is the mass of the central object in solar mass units,  $\dot{m} = \dot{M}/\dot{M}_{\text{Edd}}$  is the accretion rate in Eddington units ( $\dot{M}_{\text{Edd}} = 1.39 \times 10^{18} m \text{ g s}^{-1}$ ), and  $r = R/R_S$  is the local radius in Schwarzschild units ( $R_S = 2.95 \times 10^5 m \text{ cm}$ ). Here  $B_0$  is the strength of the large-scale magnetic field,  $\beta$  is assumed to be independent of  $R$  and takes, likely, sub-equipartition values ( $\beta \gtrsim 1 - 10$ ),  $\rho_p/R$  is the proton Larmor scale in terms of the local scale of the accretion flow, and  $v_r/c$  and  $v_A/c$  are the radial inflow velocity and the non-relativistic Alfvén speed,<sup>6</sup> respectively, in units of the speed of light.

The electron temperature is nearly constant throughout the accretion flow and starts to decrease at large radii,  $r \gtrsim 10^2 - 10^3$ . The efficient cooling of relativistic electrons prevents higher temperatures at smaller radii. Thus the proton-to-electron temperature ratio ranges from  $T_p/T_e \sim 10^3$  deeply inside the flow at  $R \sim \text{few} \times R_S$  to  $T_p/T_e \sim 1$  in the outer regions,  $R/R_S \gtrsim 10^3$ .

The MHD turbulence in hot, collisionless accretion flows is likely to originate as a result of the magneto-rotational instability (Balbus & Hawley 1991). In the linear phase, the Balbus-Hawley instability predominantly amplifies the toroidal component of the large-scale magnetic field, so that the fluctuations are weak,  $\tilde{B} \ll B_0$ . When the instability reaches nonlinear amplitudes, it becomes large scale,  $k_{BH} \sim R^{-1}$ , so that long wavelength MHD waves are excited and the MHD turbulence results, as seen from numerical simulations (see, e.g., a review by Balbus & Hawley 1998 and references therein). This turbulence is generated on large scales and, hence, carries most of the gravitational potential energy of the accreting gas. Since the ADAF gas/plasma is two-temperature, with the protons much hotter than the electrons, all compressional MHD modes are heavily damped by the collisionless (Landau and transit time) damping and thus are hard to excite, as suggested by Quataert (1998). Thus, only noncompressive (Alfvén) MHD modes may be efficiently excited and reach nonlinear amplitudes. The nonlinear saturation of the Balbus-Hawley instability means that the local fluctuating magnetic fields in the accretion flow become comparable to the averaged global magnetic field and prevent its further growth; thus in the absence of dissipation<sup>7</sup>  $\tilde{B}/B_0 \sim 1$ . At such amplitudes, noncompressibility of Alfvén waves is no longer a good approximation and the nonlinear theory of strong MHD turbulence discussed in the previous section should be used instead. In this case, Landau damping will decrease the amplitude of turbulence to a level when dissipation balances energy input. Given the noise properties, the amplitude of turbulence may be estimated from Medvedev & Diamond (1997).

### 3.2. Dissipation-dominated parallel cascade

As we discussed in the previous section (§2), there is a regime of strong nonlinear Alfvénic turbulence in which all energy that is injected into a system on large scales dissipates in the cascade and does not reach the proton Larmor radius scales. The bifurcation point, which is given by Eq.

<sup>6</sup>In the relativistic case, the displacement current cannot be neglected in Maxwell's equations. The relativistic Alfvén velocity then reads  $v_A^{\text{rel}} = v_A/\sqrt{1+v_A^2/c^2}$ . We neglect this relativistic effect in our paper because it may be significant very close to the inner edge of the flow, near the last stable orbit,  $r \sim 3$ , only.

<sup>7</sup>This condition does not place any constraint on the value of  $B_0$ .

(3), is a function of  $T_p/T_e$  and  $\beta$ , only (via  $N_1$  and  $N_2$ , see Appendix). It is independent of the fluctuation level  $b \propto \tilde{B}/B_0$  because steepening and damping are both cubic in  $b$  and the wave amplitude cancels out. (The rate of dissipation, however, does depend on the amplitude of turbulence, as discussed below in §4.1.) Using the expressions for  $N_1$  and  $N_2$  given in Appendix and Eq. (3), we now plot the borderline between the two regimes, as a function of plasma parameters.

The  $T_p/T_e$ - $\beta$ -diagram of state of the nonlinear Alfvénic turbulence is shown in Fig. 1. The shaded region corresponds to  $|N_1/N_2| < 1.3$  and the unshaded region — to  $|N_1/N_2| > 1.3$ . The bold-faced part of the boundary curve represents the range of the temperature ratio relevant for ADAFs:  $T_p/T_e$  decreases from  $\sim 10^3$  in the inner regions of the accretion flow at radii  $R \lesssim 10R_S$  to  $\sim 1$  in the outer regions at  $R \gtrsim 10^2 - 10^3 R_S$ . As is seen from the figure, the boundary between the two phases of turbulence is insensitive to the temperature ratio for the ADAF conditions and set only by plasma  $\beta$ . If  $\beta > \beta_{\text{crit}} \simeq 2.6$ , the Alfvénic turbulence in an ADAF is in the regime in which the parallel cascade is strongly dissipative. If additionally the parallel cascade is dominant (i.e., faster than any other cascade/dissipation process), then it dissipates all injected energy. Alternatively, for  $\beta < \beta_{\text{crit}} \simeq 2.6$ , Alfvén wave energy does not dissipate in the parallel cascade (even if it is dynamically dominant) and reaches  $k_{\parallel} \sim \rho_p^{-1}$  where it may be dissipated by other mechanisms, or cascade beyond this point to even smaller scales.

### 3.3. Electron vs. proton heating in the parallel cascade

We can also investigate the electron-to-proton heating ratio,  $\delta$ , using the equations for  $N_1$  and  $N_2$  as follows. The electron and proton contributions to the wave dissipation are proportional to the imaginary part of the plasma dispersion function, Eq. (A17). The factor in Eq. (A17) with integral over the distribution function has been explicitly incorporated into the wave equation, Eq. (1), as the Hilbert operator. The numerical factor was left in the coefficients, Eqs. (A6) – (A16), and is proportional to  $e^{-X_e^2}$  and  $e^{-X_p^2}$  for the electrons and protons, respectively. By vanishing by hands all those terms which are multiplied by  $e^{-X_e^2}$ , we may easily determine how much the electrons contribute to the overall dissipation of waves. Calculating the ratio  $(1 - N_2^*)/N_2^* = \delta$ , where  $N_2^*$  is the nonlinear dissipation coupling coefficient without the contribution of the electrons to dissipation, we obtain the heating ratio. Note, that in  $N_2^*$  the electrons still contribute to the linear and nonlinear dispersion of waves, as represented by the real part of the plasma distribution function.

A contour plot showing the levels of constant heating ratio,  $\delta = .005, .01, \dots, .035$ , is superimposed onto the Alfvénic dominated dissipation region in Fig. 1. Fig. 2 also depicts the heating ratio as a function of the temperature ratio  $T_p/T_e$  for two values of  $\beta$ ,  $\beta = 3$  and 40. Clearly,  $\delta$  depends on  $\beta$  only weakly and ranges with temperature from  $\sim .025$  to  $\sim .005$  for the typical ADAF conditions.

Since, the spectral ADAF models weakly depend on  $\delta$  so long as  $\delta \lesssim \text{few} \times 10^{-2}$ , we set a conservative upper limit on the electron heating in the dissipative *parallel* cascade of nonlinear Alfvénic turbulence:

$$\delta_{\parallel} \equiv \frac{P_e}{P_p} \Big|_{\text{casc}} \lesssim .025, \quad \text{if } \beta > \beta_{\text{crit}} \simeq 2.6. \quad (5)$$

#### 4. OTHER COMPETING PROCESSES

In the previous section (§3.3) we demonstrated that the energy which heats the electrons in the compressible Alfvénic dissipative parallel cascade in typical ADAF conditions constitutes a few percents of the total energy which goes into the protons. If this parallel cascade would be the only one which operates, then equation (5) gives a solid prediction. In fact, there are other competing processes which transfer Alfvénic energy in  $k$ -space and thus may affect the energetics. We consider them in order.

In addition to the compressible parallel cascade, there is an incompressible perpendicular cascade due to direct interactions of linear Alfvén wave packets. Recently two different theories of this process have been proposed. Goldreich & Sridhar (1995) (hereafter GS) showed that 4-wave interactions lead to a critically balanced anisotropic cascade in which  $k_{\parallel}$  and  $k_{\perp}$  are uniquely related. A nice paper by Ng & Bhattacharjee (1996) (hereafter NB) demonstrates that 3-wave interactions of  $k_{\parallel} = 0$  perturbations are not empty and result in a more conventional Iroshnikov-Kraichnan-type cascade. Although there are some indications from both theoretical arguments and numerical simulations (Goldreich & Sridhar 1997; Cho & Vishniac 2000) that the GS cascade dominates over the NB cascade, the debate is still not completely resolved. For this reason, we consider both possibilities below. Briefly, we obtained that the GS cascade puts some limitations on our predictions of §3.3. The NB cascade, however, does not alter our conclusions about the electron vs proton heating, despite that the total wave energy in the perpendicular direction may be substantial.

##### 4.1. Parallel vs. GS cascade

The critically balanced GS cascade (Goldreich & Sridhar 1995) is an anisotropic, (almost) perpendicular cascade in which  $k_{\parallel} \ll k_{\perp} \propto k_{\parallel}^{3/2}$ . This cascade involves linear Alfvén waves and, thus, is independent of the amplitude of the turbulence. No damping occurs in this process. The MHD (Alfvén) energy is transferred from the scales where it is injected,  $k_{\perp i} \sim R^{-1}$ , to the scales where it is dissipated or converted into other waves,  $k_{\perp f} \sim \rho_p^{-1}$ . We have to compare it with the competing compressible parallel cascade during which much of injected energy is dissipated. The rate of the energy transfer depends on the turbulence level via the compressibility. Since these two cascade processes are independent (at least in the KNLS approximation), we may compare relative contribution of each of them to the electron heating as a function of the amplitude of MHD turbulence in ADAFs.

The characteristic rate (i.e., the inverse  $e$ -folding time) of the GS cascade is the Alfvénic frequency,  $\gamma_{\text{GS}} \sim \omega_A$ . The characteristic dissipation rate in the parallel cascade

and the nonlinear cascade rate itself are comparable and estimated from Eq. (1) to be  $\gamma_{\text{NL}} \sim \omega_A |N_2| |\widetilde{b}|^2$ . Note, although the rate of the GS cascade,  $\gamma_{\text{GS}} \propto k_{\parallel}$ , increases with  $k_{\parallel}$ , so does the energy dissipation rate. Thus, the total energy dissipated in the cascade is determined by the width of the “inertial range,”  $R^{-1} \lesssim k \lesssim \rho_p^{-1}$ . The energy dissipation rate is, by definition,

$$\frac{d\epsilon}{dt} = \frac{d\epsilon}{dk_{\parallel}} \frac{dk_{\parallel}}{dt} = -\gamma_{\text{NL}} \epsilon. \quad (6)$$

Using the definition for the total energy cascade rate,  $dk_{\parallel}/dt = (\gamma_{\text{GS}} + \gamma_{\text{NL}})k_{\parallel}$ , and integrating the resultant equation, we obtain

$$\frac{\ln \epsilon/\epsilon_0}{\ln k_{\parallel m}/k_{\parallel 0}} = -\frac{|N_2| |\widetilde{b}|^2}{|N_2| |\widetilde{b}|^2 + 1}, \quad (7)$$

where  $\epsilon_0$  and  $k_{\parallel 0}$  are initial values. The largest scale is set by the size of the accretion flow,  $k_{\parallel 0} \simeq R^{-1}$ . The smallest scale is estimated from the scaling,  $k_{\parallel} \simeq k_{\perp}^{2/3} R^{-1/3}$ , of the GS cascade with  $k_{\perp m} \sim \rho_p^{-1}$ .<sup>8</sup> Thus,  $k_{\parallel m}/k_{\parallel 0} \simeq (R/\rho_p)^{2/3}$ . Quataert & Gruzinov (1999) argue that much of the energy dissipated at  $k_{\perp} \sim \rho_p^{-1}$  may heat electrons, depending on the value of  $\beta$  and numerical constants estimated from numerical simulations which are not very well constrained. We assume here the *worst* possible case in which *all the wave energy* reaching the Larmor scale heats electrons.

For the electron heating to dominate by the compressible cascade, the amount of energy that reaches the Larmor scale must be smaller than the fraction of energy that is dissipated on electrons in the compressible cascade:

$$\epsilon(k_{\parallel m})/\epsilon_0 < \delta_{\parallel}, \quad (8)$$

where  $\delta$  is given by Eq. (5). Combining all together, this inequality may now be re-written as follows:

$$|\widetilde{b}|^2 > -\frac{1}{|N_2|} \frac{\frac{3}{2} \ln \delta_{\parallel} / \ln(R/\rho_p)}{1 + \frac{3}{2} \ln \delta_{\parallel} / \ln(R/\rho_p)}. \quad (9)$$

The nonlinear coupling to dissipation,  $N_2$ , depends on plasma parameters. The dependence of  $|N_2|$  vs.  $\beta$  for two values of the proton-to-electron temperature ratio:  $T_p/T_e = 1, 10^3$  is shown in Fig. 3. Clearly, it weakly depends on  $T_p/T_e$  and is roughly  $\propto \sqrt{\beta}$ . To estimate the lower bound on  $|b|$ , we take the *lowest* value of  $|N_2| \sim 1$  for  $\beta \sim 3$ , i.e., near the bifurcation value. The normalized amplitude may be written in a general case as follows (see §2.2):

$$\begin{aligned} |\widetilde{b}|^2 &= (\tilde{B} + B_0 k_{\perp}/k)^2/B_0^2 - \langle (\tilde{B} + B_0 k_{\perp}/k)^2/B_0^2 \rangle \\ &= (\tilde{B}/B_0)^2 - \langle (\tilde{B}/B_0)^2 \rangle + 2(\tilde{B}/B_0)k_{\perp}/k \\ &\sim 2(\tilde{B}/B_0) \end{aligned} \quad (10)$$

for  $\tilde{B} \lesssim B_0$  and an oblique and nearly perpendicular angle of propagation,  $k_{\perp} \sim k$ . We take [see Eqs. (5) and

<sup>8</sup>Note, here we set a lower limit on  $k_{\parallel m}$ . Since both cascades proceed independently,  $k_{\parallel m}$  may only be larger (i.e., closer to  $\rho_p^{-1}$ ) due to the parallel cascade.

(4)]  $\delta \lesssim 2.5 \times 10^{-2}$  and  $\rho_p/R \gtrsim 6 \times 10^{-9}$ . Then the conservative limit on the fluctuation amplitude of MHD turbulence at which the electron heating is dominated by the compressible cascade is readily estimated as

$$\frac{\tilde{B}}{B_0} \gtrsim 0.2. \quad (11)$$

Thus, for  $\tilde{B}/B_0 \sim 0.2$ , the electron heating due to the parallel,  $\delta_{\parallel}$ , and perpendicular,  $\delta_{\perp}$ , cascades are of comparable value and the total electron heating is  $\delta = \delta_{\parallel} + \delta_{\perp} \sim 0.05$ . Hence, for the levels of turbulence which are believed to exist in ADAFs,  $\tilde{B}/B_0 \sim 1$ , the heating of electrons is dominated by the compressible cascade by at least an order of magnitude and yields  $\delta \lesssim 0.025$ , provided  $\beta > \beta_{\text{crit}} \simeq 2.6$ .

#### 4.2. Parallel vs. NB cascade

In a similar way we consider competition of the NB and parallel cascades. The NB cascade (Ng & Bhattacharjee 1996) proceeds in  $k_{\perp}$  only, hence it is totally independent of  $k_{\parallel}$ . There is no dissipation during the NB cascade. The Alfvén wave energy may be damped only when it reaches the  $k_{\perp} \sim \rho_p^{-1}$  scale and, as discussed in §4.1, will predominantly heat the electrons. To estimate the energy lost via the NB cascade, it is sufficient to compare the rate,  $\gamma_{\text{NB}}(\rho_p^{-1})$ , of the NB cascade at  $k_{\perp} \sim \rho_p^{-1}$  to the maximum damping rate in the  $k_{\parallel}$  cascade,  $\gamma_{\text{NL,max}}$ . The latter is  $\gamma_{\text{NL,max}} \sim \omega_{A,max} |N_2| |\widetilde{b}|^2 \sim v_A \rho_p^{-1} |N_2| |\widetilde{b}|^2$ . The former is estimated from Ng & Bhattacharjee (1996) as follows. The energy transfer rate is

$$\dot{\epsilon} \sim v^2/(N\tau) \sim \text{constant}, \quad (12)$$

where  $v^2 \sim E_k k$  is the energy per unit mass,  $N \sim (\delta v/v)$  is the number of interactions,  $\tau \sim (\kappa_{\parallel} v_A)^{-1}$  is the interaction time,  $\delta v$  is the perturbation, and  $\kappa_{\parallel}$  is a longitudinal scale of interacting Alfvén wave packets. Therefore,

$$\begin{aligned} \gamma_{\text{NB}} &\sim (N\tau)^{-1} \sim \dot{\epsilon}/v^2 \sim \dot{\epsilon}(E_k k)^{-1} \\ &\sim (E_{k0} k_0)^{-1} \left(\frac{k}{k_0}\right)^{1/2} \sim \left(\frac{\delta v_0}{v_0}\right)^2 \kappa_{\parallel 0} v_A, \end{aligned} \quad (13)$$

where we used the NB scaling  $E_k \propto k^{-3/2}$  and the subscript “0” denotes quantities at the outer scale of the turbulence. Assuming strong turbulence,  $\delta v_0 \sim v_0$ , we obtain an upper limit on  $\gamma_{\text{NB}}$ . Assuming also that on the outer scale  $k_0 \sim \kappa_0 \sim \kappa_{\parallel 0} \sim \kappa_{\perp 0} \sim R^{-1}$ , we have

$$\gamma_{\text{NB}}(\rho_p^{-1}) \sim v_A (\kappa_0 k)^{1/2} \Big|_{k \sim \rho_p^{-1}} \sim v_A (R \rho_p)^{-1/2}. \quad (14)$$

Thus, the ratio is

$$\frac{\gamma_{\text{NB}}(\rho_p^{-1})}{\gamma_{\text{NL,max}}} \sim \left(|N_2| |\widetilde{b}|^2\right)^{-1} \left(\frac{\rho_p}{R}\right)^{1/2} \sim 10^{-4}. \quad (15)$$

Thus, even if all the energy cascaded in  $k_{\perp}$  heats the electrons, it constitutes about  $10^{-4}$  of the total energy dissipated on the protons (unless  $\tilde{B}/B_0 \ll 1$ ), i.e., is completely negligible compared to equation (5). Note that the above result means only that the NB cascade is “slower” than the parallel cascade, while the total wave energy in  $k_{\perp}$  may be non-negligible.

#### 4.3. Proton-cyclotron damping vs. perpendicular cascade

The nonlinear interaction of finite-amplitude wave-packets results in generation of high- $k$  harmonics, as discussed in §2.2. Such a cascade transfers wave energy along the local magnetic field to high  $k_{\parallel}$ , where the cyclotron resonance,  $\omega - k_{\parallel} v - \Omega_p = 0$ , may be satisfied and the cyclotron damping on (bulk) protons becomes very efficient. This effect was completely missing from previous studies because both the GS and NB cascades are (nearly) perpendicular;  $k_{\parallel}$  is always small, so that only a very small number of particles from the tail of a particle distribution function are in the resonance. The proton-cyclotron damping is known to heat protons only, no energy goes to electrons, since  $\Omega_p \ll \Omega_e$  and electrons are off resonance. It is, however, difficult to rigorously estimate the  $|\widetilde{b}|^2$ , because for the cyclotron damping to dominate, it must be faster than the typical GS or NB cascading time, i.e.,  $\gamma_c \gtrsim \omega_A$ . Such a situation may occur only when  $\omega_A \simeq \Omega_p$ , so that (i) Alfvén waves are heavily damped and (ii) they may convert to proton cyclotron waves, which greatly complicates a rigorous analysis.

One can, however, roughly estimate the fluctuation level at which the proton-cyclotron damping is so strong that most of the wave energy dissipates on protons and does not convert into whistlers. The parallel cascade proceeds until it hits a scale where the nonlinear steepening is balanced by the wave dispersion [last term in Eq. (1)]. Thus, the maximum parallel wave-number to which wave energy cascades in the compressible cascade is readily estimated from Eq. (1) to be  $k_{\parallel \text{max}} \sim |\widetilde{b}|^2 (2\Omega_p/v_A |N_{1,2}|)$ , where  $|N_{1,2}|$  is the maximum of  $|N_1|$  and  $|N_2|$ . The proton-cyclotron damping is strong when  $\omega_A = k_{\parallel} v_A \simeq \Omega_p$ . Thus, if  $k_{\parallel \text{max}} \gtrsim \Omega_p/v_A$ , the MHD turbulence heats protons only. This occurs when

$$\frac{\tilde{B}}{B_0} \gtrsim \frac{1}{4|N_{1,2}|}, \quad (16)$$

where we again took  $|\widetilde{b}|^2 \simeq 2(\tilde{B}/B_0)$ . Here  $|N_{1,2}| \sim 1$  for  $\beta \sim 3$  and increases with  $\beta$  and weakly with  $T_p/T_e$  as shown in Fig. 3. For a range of  $\beta$ 's,  $1 \lesssim \beta \lesssim 2.6$ , i.e., above the bifurcation threshold (dissipation in the compressible cascade is weak), but below equipartition, the conservative condition on  $\tilde{B}$  reads:

$$\frac{\tilde{B}}{B_0} \gtrsim 0.3. \quad (17)$$

#### 4.4. Is nonlinear trapping important?

The parallel (coherent) cascade of the wave energy occurs due to the formation and nonlinear evolution of coherent wave structures, such as shocks, Alfvénic discontinuities, solitary wave-packets, etc., as discussed in §2.2. The resonant particles, i.e., those which take the energy from waves and result in damping, turn out to be trapped in the wave potential created by the wave magnetic field. Those resonant particles which move a little slower than the wave will be reflected from the rear part of the wave

potential, gain energy, and start to move faster than the wave. The particles moving faster than the wave will be reflected from the front part of the wave potential and, correspondingly, give energy to the wave and decelerate. Upon a half bounce time,  $\tau_b/2$ , the particles which have been reflected from the rear of the potential cross through it and reach its front part, where they are reflected back and give their energy to the wave. The slow particles do the opposite at the rear part. Such a process may repeat over and over again, provided the wave amplitude is maintained constant by an external source (e.g., the Balbus-Hawley instability in ADAFs), to prevent particles from escape. Clearly, the number of slow ( $v < v_A$ ) and fast ( $v > v_A$ ) particles will oscillate with time, so that the wave damping rate will change in time too and may become negative (i.e., the wave amplitude will grow) during some periods of time. The bounce period of a particle depends on its energy, because a wave trapping potential is, in general, anharmonic. Due to the difference in the bounce periods, groups of particles with different energies gain a phase shift which grows with time. Upon many cycles (bounces), the particles near the resonance,  $v \sim v_A$ , become completely randomized in phase and form an equilibrium, *plateau* distribution. At this moment, the wave collisionless dissipation quenches.<sup>9</sup> The process described above is referred to as the nonlinear Landau damping (see Medvedev et al. 1998 for more details). Numerical simulations of the process show that it takes  $\sim 10^2 - 10^3 \tau_b$  or even longer for particles to phase mix and quench collisionless damping. We note here that the nonlinear Landau damping is significant for large amplitude waves  $\tilde{B}/B_0 \sim 1$ , for which the number of trapped particles may be large.

We now estimate whether particle trapping is important for the physics of ADAFs and, in particular, whether the Alfvén wave damping during the parallel (compressible) cascade in ADAFs quenches. First, the kinetic energy of a particle in a potential is of order its potential energy, so that the typical velocity of a particle of mass  $m_j$  ( $j = e, p$ ) is  $v_j \sim (\tilde{B}^2/8\pi m_j n)^{1/2} \sim v_{Aj}(\tilde{B}/B_0)$ . The typical scale of the potential,  $\lambda$ , is set by the scale at which the energy is pumped into the system, i.e., the scale of the Balbus-Hawley instability,  $\lambda \sim k_{BH}^{-1} \sim R$ . Thus the characteristic oscillation period of a particle (the bounce time) at a given radial position in the accretion flow is  $\tau_b \sim \lambda/v_j$ , which yields

$$\tau_{bp} \simeq R/(v_A \tilde{B}/B_0), \quad \tau_{be} = (m_e/m_p)^{1/2} \tau_{bp} \quad (18)$$

for protons and electrons, respectively. Second, accreting gas flows into the central object and, thus, continuously replenished with a fresh material on the outer edge of the ADAF. The typical infall time at a given radius  $R$  is

$$\tau_r \simeq R/v_r, \quad (19)$$

where  $v_r$  is the radial velocity of a gas given by Eqs. (4). Estimating the number of bounces of a particle of species  $j$  in an Alfvén wave at a radial position  $R$  as  $\mathcal{N}_j(R) \sim \tau_r/\tau_{bj}$ ,

we obtain

$$\mathcal{N}_p \simeq 0.4\alpha(1 + \beta)^{1/2}(\tilde{B}/B_0), \quad \mathcal{N}_e \simeq 43\mathcal{N}_p. \quad (20)$$

Note that  $\mathcal{N}$  is independent of radius. The above equations show that the protons in the accretion flow are always in the linear regime of damping (no trapping,  $\mathcal{N}_p \lesssim 1$ ). The electrons may experience up to a few tens of bounces within the infall time, which is probably not enough to quench damping on electrons at all, but still may lower its value a little. We thus conclude that the damping process in the compressible parallel cascade is hardly affected by nonlinear particle trapping and the value of  $\delta \sim \text{few} \times 10^{-2}$  represents a conservative upper limit on the the electron to proton heating ratio in hot, advection-dominated accretion flows with strong magnetic field turbulence,  $\tilde{B} \sim B_0$ .

## 5. CONCLUSIONS

The particle heating is one of the key issues for the advection-dominated accretion flow models. All the models assume that protons receive most of the energy released due to viscous (turbulent) heating of the accretion gas, while electrons remain relatively cold; hence the low luminosities of ADAFs. In the collisionless plasma of the ADAFs, particle heating is determined solely by excitation and dissipation of plasma collective motions (waves). The instability of Balbus & Hawley which is believed to operate and produce magnetic fields in such differentially rotating flows may naturally result in strong MHD turbulence with highly fluctuating magnetic fields,  $\tilde{B} \sim B_0$ , during the nonlinear stages of its evolution. A detailed analysis of particle heating by such turbulence is presented in this paper.

We show that in the most natural case of the ADAF parameters,  $\beta \gtrsim 3$  and  $\tilde{B}/B_0 \gtrsim 0.2$ , dissipation of the magnetic energy occurs predominantly in the parallel, compressible cascade (the effect absent for linear, low-amplitude Alfvén waves). Most of the dissipated energy heats protons, while electrons receive only  $\delta \sim \text{few}\%$  of the energy, which in agreement with the empirical values inferred from the spectral fits for various, low-luminosity accreting systems. If, alternatively, the magnetic field in ADAFs is close to equipartition,  $\beta \lesssim 3$ , the energy of MHD turbulence is dissipated only on protons via the cyclotron damping mechanism, provided the amplitude of the turbulence is somewhat higher,  $\tilde{B}/B_0 \gtrsim \text{few} \times 10^{-1}$ . The electron heating is negligible in this case. At lower amplitudes, however, the nonlinear effects are weak and the results of the linear analysis for the dissipation of the linear Alfvén waves, addressed by other authors, hold.

The author is grateful to Ramesh Narayan for his interest in this work and helpful discussions, to the referee Amitava Bhattacharjee for many insightful comments and suggestions which helped to greatly improve the manuscript and stimulated further work, and to Eliot Quataert for discussions. This work was supported by NASA grant NAG 5-2837 and NSF grant PHY 9507695.

## APPENDIX

<sup>9</sup>This process does not affect the cyclotron damping on protons, which operates at the cyclotron, and not Cherenkov, resonance.



EXACT FORMULAE FOR THE NONLINEAR COEFFICIENTS  $N_1$  AND  $N_2$ 

The nonlinear coefficients in Eq. (1) has been calculated from the full kinetic treatment by solving the Vlasov equation for arbitrary wave profile and determining the wave-induced plasma density perturbation (Spangler 1989, 1990). They are

$$N_1 = M_1 - m_1, \quad N_2 = M_2 - m_2, \quad (\text{A1})$$

where  $M_1$  and  $M_2$  are the isotropic pressure contributions and  $m_1$  and  $m_2$  are the contributions due to pressure anisotropy (i.e., the temperatures and, hence, pressures may be different along the ambient magnetic field and perpendicular to it,  $p_{\parallel} \neq p_{\perp}$ ):

$$M_1 = -\frac{1}{4} \left( f_7 + \frac{f_5 (f_1 f_2 - \pi f_3 f_4) + \pi f_6 (f_3 f_2 + f_1 f_4)}{(f_2^2 + \pi f_4^2)} \right), \quad (\text{A2})$$

$$M_2 = -\frac{\sqrt{\pi}}{4} \left( f_6 + \frac{f_6 (f_1 f_2 - \pi f_3 f_4) - f_5 (f_3 f_2 + f_1 f_4)}{(f_2^2 + \pi f_4^2)} \right), \quad (\text{A3})$$

$$m_1 = -\frac{1}{4X_p^2} \left( g_1 + \frac{g_4 (f_1 f_2 - \pi f_3 f_4) + \pi g_3 (f_3 f_2 + f_1 f_4)}{2(f_2^2 + \pi f_4^2)} \right), \quad (\text{A4})$$

$$m_2 = -\frac{\sqrt{\pi}}{4X_p^2} \left( g_2 + \frac{g_3 (f_1 f_2 - \pi f_3 f_4) - g_4 (f_3 f_2 + f_1 f_4)}{2(f_2^2 + \pi f_4^2)} \right), \quad (\text{A5})$$

where  $\sqrt{\pi}$  appears in numerators of  $M_2$  and  $m_2$  because the Hilbert operator carries an extra  $(1/\pi)$  and additional  $(1/2)$  in all four coefficients absorbs it from the wave equation, as compared to Spangler (1989, 1990). The coefficients  $f_1, f_2, \dots, f_7, g_1, \dots, g_4$  are defined as

$$f_1 = -X_p Z_R(X_p) + X_e Z_R(X_e), \quad (\text{A6})$$

$$f_2 = [1 + X_p Z_R(X_p)] + T_r [1 + X_e Z_R(X_e)], \quad (\text{A7})$$

$$f_3 = X_p e^{-X_p^2} - X_e e^{-X_e^2}, \quad (\text{A8})$$

$$f_4 = X_p e^{-X_p^2} + T_r X_e e^{-X_e^2}, \quad (\text{A9})$$

$$f_5 = 1 + X_p Z_R(X_p), \quad (\text{A10})$$

$$f_6 = X_p e^{-X_p^2}, \quad (\text{A11})$$

$$f_7 = X_p Z_R(X_p), \quad (\text{A12})$$

$$g_1 = [X_p^2 + X_p^3 Z_R(X_p) - X_p Z_R(X_p)] + (1/T_r)[X_e^2 + X_e^3 Z_R(X_e) - X_e Z_R(X_e)], \quad (\text{A13})$$

$$g_2 = (X_p^3 - X_p) e^{-X_p^2} + (1/T_r)(X_e^3 - X_e) e^{-X_e^2}, \quad (\text{A14})$$

$$g_3 = (2X_p^3 - X_p) e^{-X_p^2} - (2X_e^3 - X_e) e^{-X_e^2}, \quad (\text{A15})$$

$$g_4 = [2X_p^2 + 2X_p^3 Z_R(X_p) - X_p Z_R(X_p)] - [2X_e^2 + 2X_e^3 Z_R(X_e) - X_e Z_R(X_e)]. \quad (\text{A16})$$

Here  $Z_R(X)$  is the real part of the plasma dispersion function for argument  $X$ :

$$Z(X) = \frac{1}{\sqrt{\pi}} \int_{-\infty}^{\infty} \frac{\exp(-\xi^2)}{\xi - X} d\xi = 2i e^{-X^2} \int_{-\infty}^{iX} e^{-\xi^2} d\xi. \quad (\text{A17})$$

The imaginary part of  $Z(X)$  appears explicitly in Eq. (1) as the Hilbert integral operator. Physically,  $X = X_R + iX_I$  is the ratio of wave phase velocity to thermal velocity. For Alfvén waves,  $X_p$  and  $X_e$  become:

$$X_p = \left(1 + \frac{T_e}{T_p}\right)^{1/2} \frac{1}{\sqrt{\beta}}, \quad X_e = \left(\frac{T_p}{T_e} + 1\right)^{1/2} \sqrt{\frac{m_e}{m_p}} \frac{1}{\sqrt{\beta}} \quad (\text{A18})$$

At last,  $T_r = T_p/T_e$  is the proton-to-electron temperature ratio and  $m_e/m_p \simeq 1/1836$  is the electron-to-proton mass ratio.

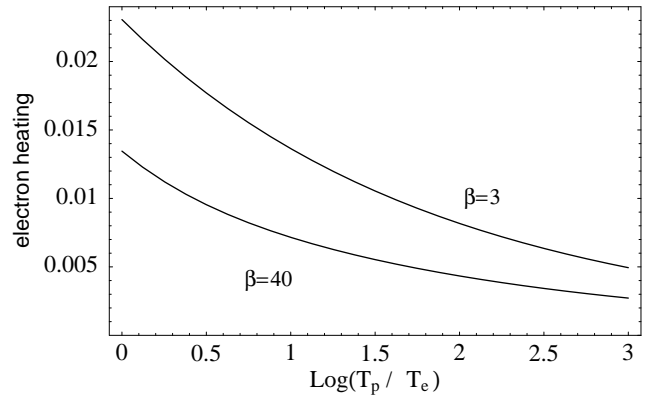
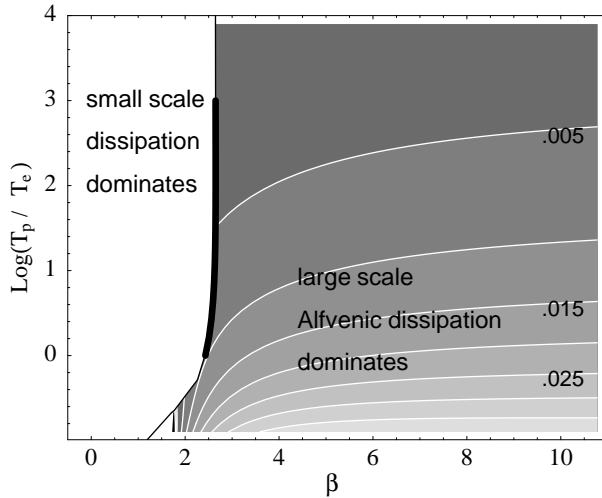
## REFERENCES

- Abramowicz, M., Chen, X., Granath, M., & Lasota, J. P. 1996, *ApJ*, 471, 762
- Balbus, S. A., & Hawley, J. F. 1991, *ApJ*, 376, 214
- Balbus, S. A., & Hawley, J. F. 1998, *Rev. Mod. Phys.*, 70, 1
- Begelman, M. C., & Chiueh, T. 1988, *ApJ*, 332, 872
- Bisnovatyi-Kogan, G. S., & Lovelace, R. V. E. 1997, *ApJ*, 486, L43
- Blandford, R. D. & Begelman, M. C. 1999, *MNRAS*, 303, L1
- Cho, J., & Vishniac, E. T. 2000, *ApJ*, accepted (astro-ph/0003403)
- Cohen, R. H., & Kulsrud, R. M. 1971, *Phys Fluids*, 17, 2215
- Di Matteo, T., Fabian, A. C., Rees, M. J., Carilli, C. L., & Ivison, R. J. 1999, *MNRAS*, 305, 493
- Gammie, C. F., Narayan, R., & Blandford, R. 1999, *ApJ*, 516, 177
- Gruzinov, A., & Quataert, E. 1999, *ApJ*, 520, 849
- Goldreich, S., & Sridhar, S. 1995, *ApJ*, 438, 763
- Goldreich, S., & Sridhar, S. 1997, *ApJ*, 485, 680
- Hameury, J. M., Lasota, J. P., McClintock, J. E., & Narayan, R. 1997, *ApJ*, 489, 234
- Ichimaru, S. 1977, *ApJ*, 214, 840
- Lasota, J. P., Abramowicz, M., Chen, X., Krolik, J., Narayan, R., & Yi, I. 1996, *ApJ*, 462, 142
- Mahadevan, R. 1997, *ApJ*, 477, 585
- Mahadevan, R. 1998, *Nature*, 394, 651
- Manmoto, T., Mineshige, S., & Kusunose, M. 1997, *ApJ*, 489, 791
- Medvedev, M. V. 1999, *Phys. Plasmas*, 6, 2191
- Medvedev, M. V., Diamond, P. H., Rosenbluth, M. N., & Shevchenko V. I., 1998, *Phys. Rev. Lett.*, 81, 5824
- Medvedev, M. V., & Diamond, P. H. 1997, *Phys. Rev. E*, 56, R2371
- Mjølhus, E., & Wyller, J. 1988, *J. Plasma Phys.*, 40, 299
- Narayan, R., Barret, D., & McClintock, J. E. 1997, *ApJ*, 482, 448
- Narayan, R., Mahadevan, R., Grindlay, J. E., Popham, R. G., & Gammie, C. F. 1998, *ApJ*, 492, 554
- Narayan, R., Mahadevan, R., & Quataert, E. 1998, in *The Theory of Black Hole Accretion Discs*, eds. M. A. Abramowicz, G. Bjornsson, and J. E. Pringle (Cambridge: Cambridge University Press)
- Narayan, R., & Yi, I. 1995, *ApJ*, 452, 710
- Narayan, R., Yi, I., & Mahadevan, R. 1995, *Nature*, 374, 623
- Ng, C.S., & Bhattacharjee, A. 1996, *ApJ*, 465, 845
- Oraevskii, B. N. 1983, in *Basic plasma physics*, Vol. 1, ed. A. A. Galeev & R. N. Sudan (New York : North-Holland Pub.), 241
- Quataert, E. 1998, *ApJ*, 500, 978
- Quataert, E., & Gruzinov, A. 1999, *ApJ*, 520, 248
- Quataert, E., & Narayan, R. 1999, *ApJ*, 520, 849
- Rees, M. J., Begelman, M. C., Blandford, R. D., & Phinney, E. S. 1982, *Nature*, 295, 17
- Reynolds, C. S., Di Matteo, T., Fabian, A. C., Hwang, U., & Canizares, C. R. 1996, *MNRAS*, 283, L111
- Spangler, S. R. 1989, *Phys. Fluids B*, 1, 1738
- Spangler, S. R. 1989, *Phys. Fluids B*, 2, 407

FIG. 1.— A  $T_p/T_e$ - $\beta$ -diagram of state of nonlinear Alfvénic turbulence. The shaded region corresponds to the compressional cascade dominated regime (phase) of turbulence. The contour lines represent the electron-to-proton heating ratio,  $\delta$ , in MHD turbulence in ADAFs with  $\tilde{B}/B_0 \gtrsim 0.1$ . The unshaded region corresponds to the small-scale dissipation dominated phase, where the Goldreich-Sridhar cascade is dominant. The boldfaced part of the dividing (bifurcation) line corresponds to the range of the  $T_p/T_e$  parameter typical of ADAFs.

FIG. 2.— The electron-to-proton heating ratio vs.  $T_p/T_e$  for  $\beta = 3$  and  $\beta = 40$ .

FIG. 3.— The coefficients of nonlinear damping,  $|N_2|$  (solid curves), and nonlinear steepening,  $N_1$  (dashed curves), vs.  $\beta$  for two values of the temperature ratio,  $T_p/T_e = 10^3$  (boldface curves) and  $T_p/T_e = 1$  (thin curves).



Figs. 1,2

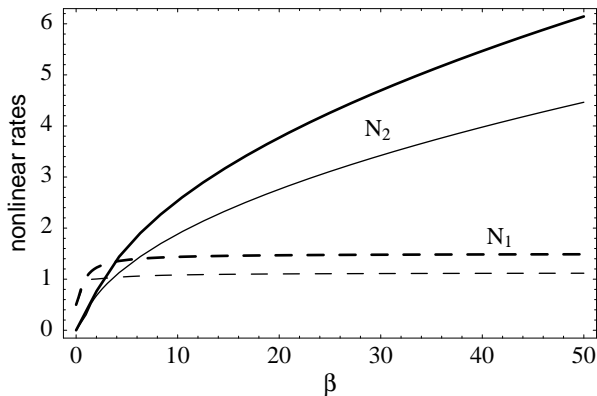


Fig. 3